

# Novel Poly(pyrrole-co-3-acetyl pyrrole)-WO<sub>3</sub> nanocomposites modified gold electrode as electrocatalytic oxidation and reduction of H<sub>2</sub>O<sub>2</sub>

Nitin Dighore<sup>id</sup>, Priya Dahare, Suresh Gaikwad, Anjali Rajbhoj\*

The fabrication of an electrochemical sensor based on novel poly(pyrrole-co-3acetyl pyrrole)-WO<sub>3</sub> nanocomposites modified gold electrode (PPAP-WO<sub>3</sub>-AuE) and its electrocatalytic oxidation and reduction of hydrogen peroxide is described here. The PPAP-WO<sub>3</sub> nanocomposites were synthesized by chemical method and characterized by different techniques. The WO<sub>3</sub> nanoparticles incorporated with PPAP were confirmed by x-ray diffraction pattern, scanning electron microscopy and transmission electron microscope micrograph. The electrochemical behaviour of PPAP-WO<sub>3</sub>-AuE towards the electro catalytic oxidation and reduction of hydrogen peroxide was investigated by cyclic voltammetry, differential pulse voltammetry and square wave voltammetry. The observed DPVs and SWVs response depend linearly on concentration of hydrogen peroxide in the range of 1-10 mM and with limit of detection (LOD) is  $1 \times 10^{-4}$  M. The correlation coefficients were found as 0.991, 0.930 and sensitivity observed was  $47.64 \mu\text{A}/\text{mM}\cdot\text{cm}^2$  and  $8.31 \mu\text{A}/\text{mM}\cdot\text{cm}^2$ . These results indicate the PPAP-WO<sub>3</sub>-AuE exhibited good platform and could be used for electrochemical determination of hydrogen peroxide.

## Introduction

Hydrogen peroxide have strong oxidizing property hence widely used as oxidizing agent in various food production, organic compound synthesis, pulp & paper bleaching, sterilization, clinical application, pharmaceutical and environmental analysis [1-4]. H<sub>2</sub>O<sub>2</sub> is by product of the most of the oxidative biological reactions which is most important factor of diseases like cancer, asthma, neurodegenerative disorder heart diseases [5-8] etc. Hence the detection and quantification of H<sub>2</sub>O<sub>2</sub> was based on a simple credible, precise, fast & economical. Several methods have been developed for qualitative and quantitative detection of H<sub>2</sub>O<sub>2</sub> such as titration [9], spectrophotometry [10], chemiluminescence [11], fluorometric [12] and chromatographic [13] techniques. But most of the methods have disadvantage like high cost,

time consuming, and complexity while electrochemical methods have preferably low cost, high efficiency, sensitivity, selectivity [14] and reproducibility of electrode in operation.

Recent studies on various polymer nanocomposites were used as electrochemical biosensor [15], drugs sensor [16,17], an environmental pollutant sensor [18], water and soil sample analysis [19], pharmaceutical and human fluids [20].

Several nanocomposites based modified electrode such as Pt Nanoparticle-Decorated rGO-CNT Nanocomposite [21], poly(azureA)-platinum nanoparticles [22], Co-embedded N-doped hierarchical carbon [23], Ag-Au / RGO / TiO<sub>2</sub> nanocomposite [24], Co<sub>3</sub>O<sub>4</sub> nanowall [25], novel metals [26-28] and conducting polymer nanocomposites [29,30] have been used for direct oxidation, reduction and detection of H<sub>2</sub>O<sub>2</sub>. In the present study chemically synthesized novel PPAP-WO<sub>3</sub> nanocomposites (NCPs) for the electrochemical detection of H<sub>2</sub>O<sub>2</sub> has newer approach. In the present observation we have adapted electrochemical detection of H<sub>2</sub>O<sub>2</sub> by cyclic voltammetry (CV), differential pulse voltammetry (DPV) and square wave voltammetry (SWV) techniques.

Department of Chemistry, Dr. Babasaheb Ambedkar Marathwada University, Aurangabad 431004, Maharashtra, India

\*Corresponding author:

E-mail: anjali.rajbhoj@gmail.com; Tel.: (+91) 240-2403311

DOI: 10.5185/aml.2021.15703

## Experimental

### Materials

Pyrrole (Alfa Aesar), 3 Acetyl Pyrrole (Alfa Aesar), ferric chloride (SD-Fine Chem.), sodium tungstate dihydride ( $\text{NaWO}_4 \cdot 2\text{H}_2\text{O}$ ) (Sigma-Aldrich), oxalic acid (SD-Fine chem.), Ascorbic acid (Alfa Aesar), NaOH (Sigma - Aldrich) and Nafion D-521 dispersion (Alfa Aesar) were purchased and used as such as without further purification. All solutions were prepared in double distilled water.

### Synthesis of novel Poly(Pyrrole-co-3 acetyl Pyrrole) (PPAP)- $\text{WO}_3$ Nanocomposites

The monomer pyrrole (3 mmol) and 3-acetyl pyrrole (3 mmol) were dissolved separately in 5 ml chloroform mixed in beaker and stirred for 30 min at room temperature. The doping of pre synthesized  $\text{WO}_3$  NPs in monomer mixture solution was done by addition of 500 mg  $\text{WO}_3$  nanoparticles in mixture of pre-stirred pyrrole and 3-acetyl pyrrole solution. The monomer mixture solution was stirred for 30 min at room temperature. Then tri chloro acetic acid (TCA) (13 mmol) in 2 ml chloroform was added drop wise to the monomer solution at room temperature to start polymerization. Trichloro acetic acid was added to the monomer and nanoparticles mixture solution, the colour changed immediately from yellowish to dark green. The polymerization was carried out for 4 hrs at room temperature after which precipitation was formed in the reaction flask. After polymerization resultant residue was washed well with water and acetone. The precipitates were stirred with 3 W% NaOH in aqueous solution for 30 min in order to remove acid catalyst. The solution was stirred with 2N HCl solution for 30 min to decrease the pH and make them acidic. The obtained green precipitate of novel PPAP- $\text{WO}_3$  nanocomposites was dried for 24 hrs at room temperature.

### Preparation of modified electrode

The gold (Au) electrode (2 mm diameter) was carefully polished using a polishing cloth with alumina slurry and then rinsed thoroughly with glass distilled water. The Au electrode was placed in ultrasound cleaner for 5 min, rinsed again with glass distilled water and allowed to dry at RT. To prepare the Au electrode modified with PPAP- $\text{WO}_3$  nanocomposites, an alcoholic solution of 0.1 % Nafion dispersion of PPAP-  $\text{WO}_3$  NCPs ( $1\text{mg mL}^{-1}$ ) was prepared and the suspension ( $5\mu\text{L}$ ) was cast on to the surface of pre-treated Au electrode. The solvent was allowed to evaporate at RT which resulted in immobilized PPAP- $\text{WO}_3$  NCPs material on the Au electrode surface.

### Characterization

The prepared materials of PPAP- $\text{WO}_3$  NCPs were characterized by Fourier Transfer Infrared spectroscopy, x-ray diffraction, Scanning Electron Microscopy and Transmission Electron Microscopy techniques. The Infra-

red spectrum was recorded on Fourier Transfer Infrared spectrophotometer [JASCO, FT-IR/4100] Japan using dry KBr as standard reference in the range of  $400\text{--}4000\text{ cm}^{-1}$ . The X-ray powder diffraction patterns of PPAP- $\text{WO}_3$  NCPs were recorded on Bruker 8D advance X-ray diffractometer using Cu K $\alpha$  radiation of wavelength =  $1.54056\text{ \AA}$ . To study the morphology PPAP- $\text{WO}_3$  NCPs were examined using Scanning Electron Microscope. The Scanning Electron Microscopy analysis was carried out with JEOL; JSM-6330 LA operated at 20.0kV and 1.0000nA. Shape, size & morphology was calculated by Transmission Electron Microscopy analysis carried out on Philips model CM200 operated at 200kV.

### Electrochemical analysis

Cyclic voltammetry (CV), differential pulse voltammetry (DPV) and square wave voltammetry (SWV) measurements were performed on a Metrohm Autolab PGSTAT128N (Metrohm B.V., Utrecht, Netherlands) having a single compartment with three electrode system containing, a saturated Ag/AgCl reference electrode, a platinum wire auxiliary electrode and a modified PPAP- $\text{WO}_3$ -Au electrode as working electrode. Hydrogen peroxide measurements were carried out at pH 7.4 in 0.1 M potassium phosphate buffer solution (PBS) at room temperature. The CV, DPV and SWV were done at different concentration of hydrogen peroxide in the range 1-10 mM. For CV measurements, the potential scan was taken from -0.90 to 1.10 V at the different scan rate in the range 25-150  $\text{mVs}^{-1}$ .

## Results and discussion

### Fourier transfer infrared spectroscopy

The PPAP- $\text{WO}_3$  NCPs powder prepared were analysed by Fourier Transfer Infrared spectrophotometer in range  $400\text{--}4000\text{ cm}^{-1}$  in Fig. 1. The peak at  $3402\text{ cm}^{-1}$  was attributed to the N-H bond while the peak at  $1624\text{ cm}^{-1}$  attributed to the C-N-C bond or the C=O group form during the PPAP polymerization. The strong peak at  $2872\text{ cm}^{-1}$  and  $2824\text{ cm}^{-1}$  were related to the aliphatic C-H vibration. On the other hand, the peaks at  $1240\text{ cm}^{-1}$  and  $996\text{ cm}^{-1}$  were due to the C-N and C-H groups in the composite spectrum respectively. In addition, the peak at  $1520\text{ cm}^{-1}$  was characteristic of a typical PPAP ring vibration.

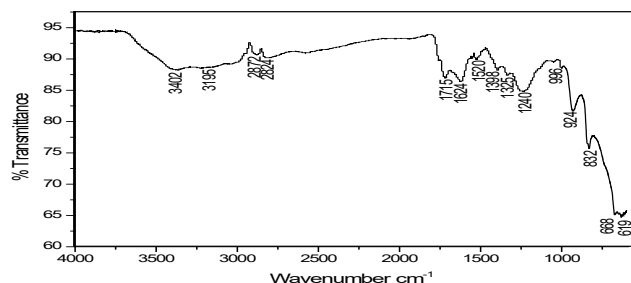


Fig. 1. Fourier Transfer Infrared spectrum of PPAP- $\text{WO}_3$  NCPs.

The Fourier Transfer Infra-red spectrum of the PPAP-WO<sub>3</sub> NCPs powder shows characteristic bipolaron bands at 1240 cm<sup>-1</sup> and broad band at 1520 cm<sup>-1</sup>, indicating the formation of PPAP in its doped state [31]. The peak at 1715 cm<sup>-1</sup> to the C=O functional group presence in indicates that the copolymerization occurred in pyrrole and 3-acetyl pyrrole. The carbonyl group frequency peak were described at 1703 cm<sup>-1</sup> in pure PPAP. After doping of WO<sub>3</sub> NPs carbonyl group frequency shifted to 1715 cm<sup>-1</sup> which indicate doping of WO<sub>3</sub> NPs. In Fourier Transfer Infra-red spectrum of PPAP-WO<sub>3</sub> NCPs sharp new peaks appears at 924 cm<sup>-1</sup>, 8320 cm<sup>-1</sup>, 668 cm<sup>-1</sup> and 619 cm<sup>-1</sup> which is the characteristic peak of WO<sub>3</sub> [32] indicating the presence of WO<sub>3</sub> in PPAP.

### X-ray diffraction

The x-ray diffraction pattern of PPAP-WO<sub>3</sub> NCPs is shown in Fig. 2. The x-ray diffraction analysis data of PPAP-WO<sub>3</sub> nanocomposites is described in Table S1, shows strong and intense peaks at 2θ (degree) = 16.41, 24.161, 25.563, 34.209, 34.880, 38.192, 45.914, 49.534, 52.612 and 56.236 corresponding to the planes of (010), (011), (111), (002), (012), (020), (301), (321), (041) (411) and (241) indicating the orthorhombic crystal structure PPAP-WO<sub>3</sub> NCPs. It was noted that all x-ray diffraction peaks are identified as WO<sub>3</sub> nanoparticles peaks from the JCPDS card No. 71-0131 with a = 7.341, b = 7.570, c = 7.754 & α = β = γ = 90. The X-ray diffraction pattern after doping of WO<sub>3</sub> nanoparticles into PPAP is shown in Fig. 2. The intercalation of WO<sub>3</sub> nanoparticles on PPAP leads to the formation to broadening peak and also decreases in peak intensity than pure WO<sub>3</sub> nanoparticles which indicate the formation of PPAP-WO<sub>3</sub> crystalline nanocomposites. The average particle size was calculated by using Debye-Scherrer formula. The PPAP-WO<sub>3</sub> NCPs showed 2θ and full width of half maximum (FWHM) which are values shown in Table S1. The average crystalline size of PPAP-WO<sub>3</sub> NCPs was found to be 13.60 nm.

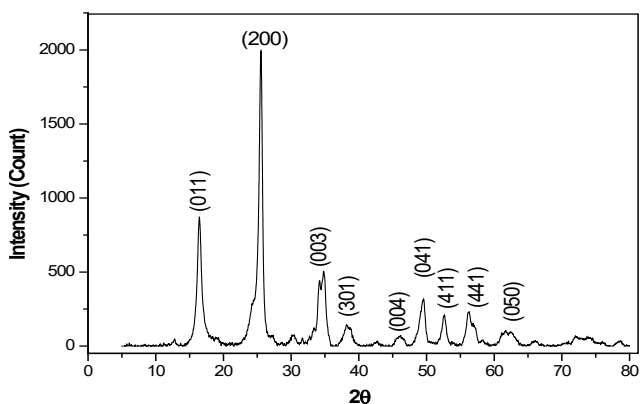


Fig. 2. XRD pattern of PPAP-WO<sub>3</sub> Nanocomposites

### Scanning electron microscopy & energy dispersive spectroscopy

The morphology of PPAP-WO<sub>3</sub> nanocomposites studied by Scanning Electron Microscope shows the micrograph of PPAP-WO<sub>3</sub> nanocomposites that are having irregular shape and their distribution is not uniform showed in Fig. 3(a). WO<sub>3</sub> nanoparticles showed agglomeration on the PPAP composites, which formed porous PPAP-WO<sub>3</sub> nanocomposites. The elemental composition of prepared PPAP-WO<sub>3</sub> nanocomposites was analysed by qualitatively and quantitatively by Energy Dispersive Spectroscopy. The elemental composition of PPAP-WO<sub>3</sub> nanocomposites by atomic % (weight %) from Fig. 3(b) were found as carbon: 55.51% (32.50%), nitrogen: 3.78% (2.58%), oxygen: 22.52% (17.57), tungstate: 2.20 (19.72) and chlorine: 15.99% (27.63) which confirmed formation of PPAP-WO<sub>3</sub> nanocomposites. The presence of chlorine was due to oxidant trichloroacetic acid used for polymerization.

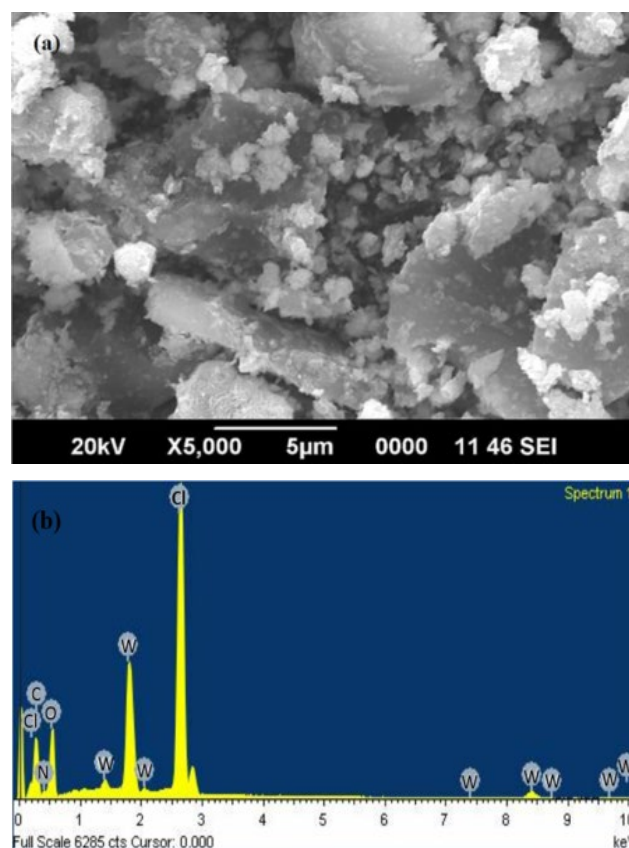


Fig. 3. (a) Scanning Electron Microscope image and (b) Energy Dispersive spectra of PPAP-WO<sub>3</sub> Nanocomposites.

### Transmission electron microscope

The Transmission electron micrograph Fig. 4(a) of PPAP-WO<sub>3</sub> nanocomposites showed that WO<sub>3</sub> nanoparticles deposited on the polypyrrole and their size was found to be 30-50 nm. The selected area electron diffraction pattern

inset of Fig. 4(a), PPAP-WO<sub>3</sub> Nanocomposites was found to be spotty ring which indicate the crystalline nature of nanocomposite. Fig. 4(c) shows a histogram of PPAP-WO<sub>3</sub> Nanocomposites, the average diameter ( $d_{\text{average}}$ ) and standard deviation ( $\sigma$ ) was found to be 36.46 nm and 13.98 respectively.

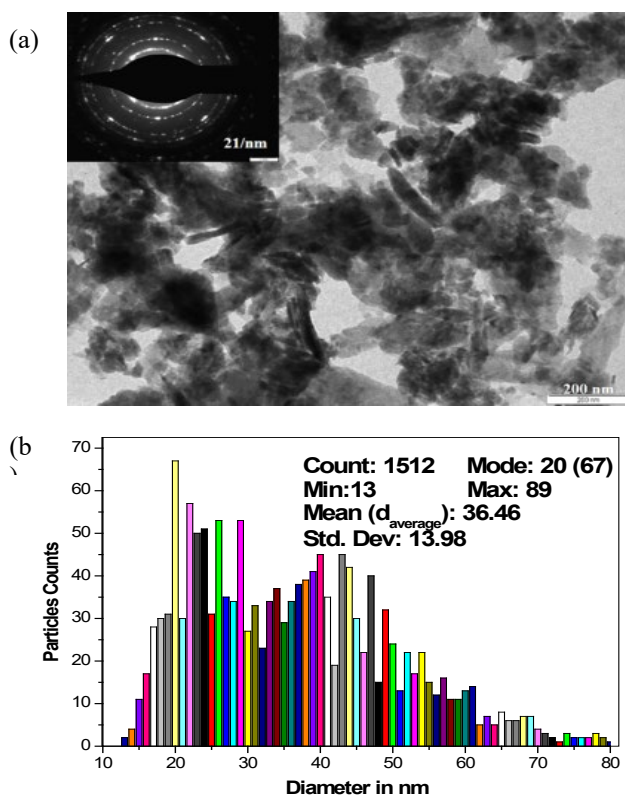


Fig. 4. (a) Transmission electron micrograph inset selected area electron diffraction pattern and (b) Histogram of PPAP-WO<sub>3</sub> nanocomposites.

#### Electrochemical behavior of PPAP-WO<sub>3</sub>-Au electrode

The electrochemical behavior of bare AuE and PPAP-WO<sub>3</sub>-AuE was studied by cyclic voltammetry of 0.1 mM potassium ferricyanide in 0.1 M KNO<sub>3</sub> at the scan rate 100 mV/s. The cyclic voltammograms show that the PPAP-WO<sub>3</sub>-AuE showed higher currents in 0.1 mM ferricyanide compared to the bare AuE. The increase peak currents are largely the result of increased electroactive surface area of the PPAP-WO<sub>3</sub>-AuE. Using diffusion coefficient  $6.8 \times 10^{-6} \text{cm}^2/\text{s}$  [33] and Randles Sevcik equation it was seen that the electroactive surface area for modified PPAP-WO<sub>3</sub>-AuE was found to be 4.5 times higher than that of bare electrode (Fig. 5(a)).

The effect of scan rate on the oxidation and reduction current on PPAP-WO<sub>3</sub>-AuE was investigated by cyclic voltammetry of 0.1 mM ferricyanide in 0.1 M KNO<sub>3</sub> at different scan rate in 25-150 mV/s in the potential range -0.2V to 0.9V (Fig. 5(b)). As shown in plot (Fig. 5(c)) from linear regression equation, the regression coefficient of

ferricyanide oxidation and reduction was with  $R^2 = 0.983$  and  $R^2 = 0.980$  respectively.

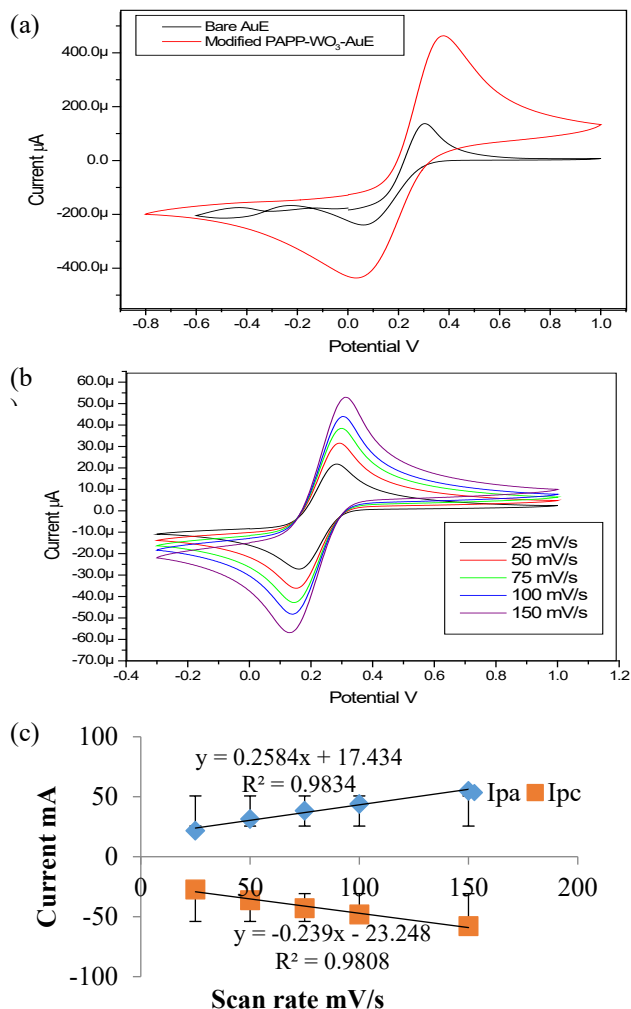


Fig. 5. CVs response of (a) bare AuE (black) and Modified electrode PPAP-AuE, (b) different scan rate 25-150 mV/s at 0.1 M potassium ferricyanide in 0.1 M KNO<sub>3</sub> (c) Linear regression curve for anodic and cathodic peak current.

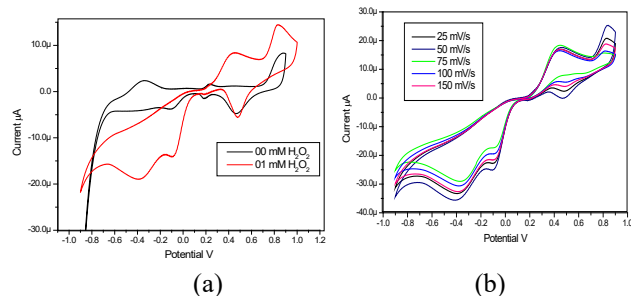


Fig. 6. (a) CV response on PPAP-WO<sub>3</sub>-AuE electrode with (Red) and Without (Black) 1 mM H<sub>2</sub>O<sub>2</sub> in 0.1 PBS at 7.4 pH. (b) CV response on PPAP-WO<sub>3</sub>-AuE electrode different scan rate 2 mM H<sub>2</sub>O<sub>2</sub> in 0.1 PBS at 7.4 pH.

Fig. 7(a) shows the obtained cyclic voltammetry at PPAP-WO<sub>3</sub>-AuE electrode for different concentration of H<sub>2</sub>O<sub>2</sub> varied from 00mM to 10 mM. The increase peak currents are

largely the result of increased electroactive surface area of the PPAP-WO<sub>3</sub>-AuE. The increase in oxidation peak current with dramatically increase in the reduction peak current increase with concentration of H<sub>2</sub>O<sub>2</sub>. As shown in plotted Fig. 6(b), from linear regression equation, the regression coefficient of oxidation and reduction was with R<sup>2</sup> = 0.988 and R<sup>2</sup> = 0.999 respectively. The sensitivity of electrode in oxidation and reduction peak was found to be 152.03 μA/mMcm<sup>2</sup> and 374 μA/mMcm<sup>2</sup> respectively.

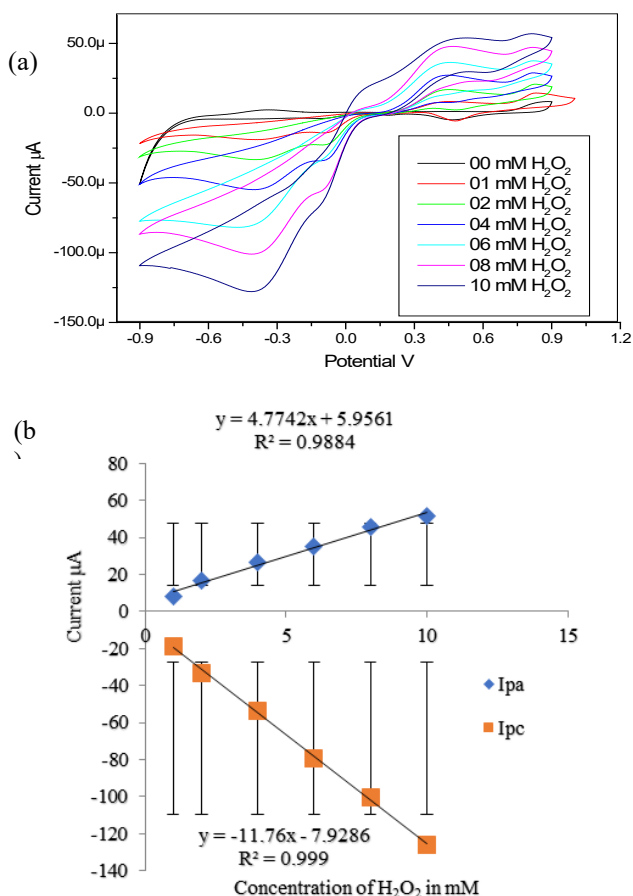


Fig. 7. (a) CVs response at PPAP-WO<sub>3</sub>-AuE in 0.1 PBS of 7.4 pH of various concentration of H<sub>2</sub>O<sub>2</sub> in 1-10 mM and (b) Linear regression curve for concentration of H<sub>2</sub>O<sub>2</sub> Vs. anodic and cathodic peak current.

### Electrochemical detection of hydrogen peroxide by differential pulse voltammetry

The voltammetric sensor using differential pulse voltammetry (DPV) was developed for the detection of hydrogen peroxide. Fig. 8(a) shows the obtained differential pulse voltammograms at PPAPy-WO<sub>3</sub>-AuE for different concentration of hydrogen peroxide. The concentration was varied from 1 mM to 10 mM in 0.1 PBS solutions at 7.4 pH. The oxidation peak current obtained was directly proportional to the concentration of hydrogen peroxide was plotted as shown in Fig. 8(b), with linear regression equation of with R<sup>2</sup> = 0.991 and the sensitivity 47.64 μA/mMcm<sup>2</sup>.

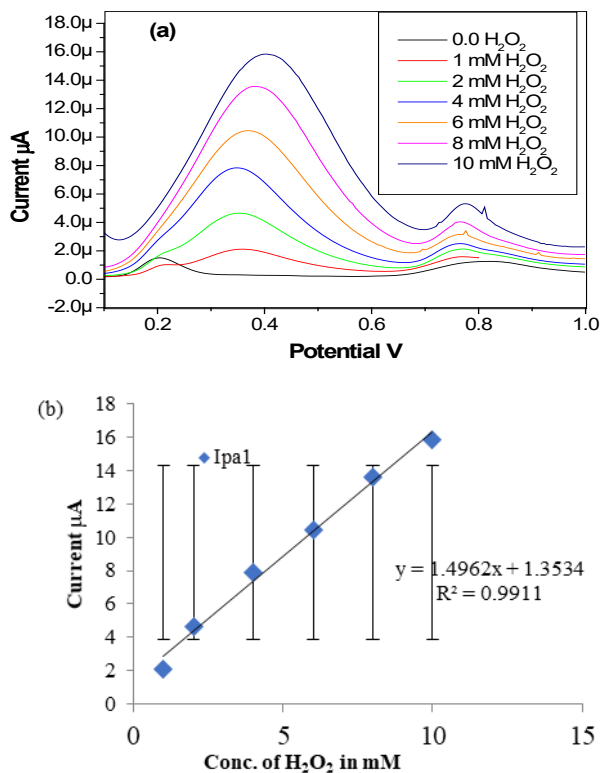


Fig. 8. (a) SWV response at PPAP-WO<sub>3</sub>-AuE in 0.1 PBS of 7.4 pH of various concentration of H<sub>2</sub>O<sub>2</sub> in 1-10 mM (b) Linear regression curve for concentration of H<sub>2</sub>O<sub>2</sub> Vs. anodic peak current.

### Conclusion

In the present study we successfully synthesized of novel PPAP-WO<sub>3</sub> nanocomposites by chemical method. The PPAP-WO<sub>3</sub> nanocomposites were crystalline, porous materials, WO<sub>3</sub> nanoparticles incorporated with PPAP and average size 30-50nm resulted from TEM analysis. The histogram was showed average size  $d_{\text{average}}$  and standard deviation ( $\sigma$ ) was found to be 36.46 nm and 13.98 respectively. The PPAP-WO<sub>3</sub> NCPs modified gold electrode was excellent used for detection of hydrogen peroxide. The CV, DPV and SWV curves resulted increase in peak current with increasing the concentration of hydrogen peroxide. The result obtained from CVs, the regression coefficient of oxidation and reduction was with R<sup>2</sup> = 0.988 and R<sup>2</sup> = 0.999 and sensitivity of electrode in oxidation and reduction peak was found to be 152.03 μA/mMcm<sup>2</sup> and 374 μA/mMcm<sup>2</sup> respectively. The observed DPVs and SWVs response depend linearly on concentration of hydrogen peroxide in the range of 1-10 mM and with limit of detection (LOD) is  $1 \times 10^{-4}$  M. The correlation coefficients were found as 0.991, 0.930 and sensitivity observed was 47.64 μA/mM.cm<sup>2</sup> and 8.31 μA/mM.cm<sup>2</sup>. These results indicate the PPAP-WO<sub>3</sub>-AuE exhibited simple, effective tool and good platform could be used for electrochemical determination of hydrogen peroxide.

### Acknowledgment

The Department of Chemistry acknowledges the financial assistance by UGC-SAP-DRS Scheme-I. One of the author NRD is thankful for financial assistance from University Scholar Fellowship, Dr. Babasaheb Ambedkar Marathwada University, Aurangabad.

### Keywords

Electro catalysis, poly(pyrrole-co-3acetylpyrrole)-WO<sub>3</sub> nanocomposites, electrochemical analysis, H<sub>2</sub>O<sub>2</sub> sensor.

Received: 8 April 2021

Revised: 27 May 2021

Accepted: 29 May 2021

### References

- Somsundaram, M.; Kirtkara K.; Tanticharoen, M.; *Anal. Chim. Acta*, **1996**, *319*, 59.
- Forzami, E. S.; Rivas, G. A.; Solis, V. M. *Journal of Electroanalytical Chemistry*, **1995**, *382*, 33.
- Kulys, J.; Gorron, I.; Domingues, I.; Emneus, J.; Jarskog, H.; *Journal of Electroanalytical Chemistry*, **1994**, *372*, 49.
- Wang, Z.; Yi, J.; Yang, S.; *Sensor and Actuator B Chemical*, **2013**, *176*, 211.
- AlObaidi, A.; *Annals of Thoracic Medicine*, **2007**, *2*, 107.
- Cai, H. L.; *Cardiovascular Research*, **2005**, *68*, 26.
- Brown, N. S.; Bicknell, R.; *Breast Cancer Research*, **2001**, *3*, 323.
- Tabner, B. J.; El-Agnaf, O. M. A.; Turnbull, S.; German, M. J.; Paleologou, K. E.; Hayashi, Y.; Cooper, N. J.; Fullwood, L. J.; Allsop, D.; *Journal of Biological Chemistry*, **2005**, *280*, 35789.
- Klassen, N.V.; Marchington, D.; McGowan; *Anal. Chem.*, **1994**, *66*, 2921.
- Tanner, P.A.; Wong, A.Y.S.; *Anal. Chim. Acta*, **1998**, *370*, 279.
- Yuan, J.C.; Shiller, A.M.; *Anal. Chem.*, **1999**, *71*, 1975.
- Taniai, T.; Sakuragawa, A.; Okutani, T.; *Anal. Sci.*, **1999**, *15*, 1077.
- Hong, J.G.; Maguhn, J.; Freitag, D.; Kettrup, A.; Fresen, J.; *Anal. Chem.*, **1998**, *361*, 124.
- Rui, Q.; Komori, K.; Tian, Y.; Liu, H.Q.; Luo, Y.P.; Sakai, Y.; *Anl. Chim. Acta*, **2010**, *670*, 57.
- Beitollahi, H.; Safaei, M.; Tajik, S.; *Anal. Bioanal. Chem Res.*, **2019**, *6*, 81.
- Shetti, N. P.; Malode, S.J.; Nayak, D. S.; Aminabhavi, M.; Reddy, K. R.; *Macrochemical Journal*, **2019**, *150*, 104124.
- Karimi-Maleh, H.; Alizadeh, M.; Orooji, Y.; Karimi, F.; Beitollahi, H.; Malekmohammadi, S.; *Indu. & Eng. Chem. Res.*, **2021**, *60*, 816.
- Tijak, S.; Beitollahi, H.; Nejad, F.; Venditti, R.; Varma, R.; Shokouhimehr, M.; *Indu. & Eng. Chem. Res.*, **2021**, *60*, 1112.
- Shetti, N. P.; Malode, S. J.; Vernekar, P.R.; Nayak, D. S.; Shetty, N. S.; Shukla, S. S.; Reddy, K. R.; Aminabhavi, M.; *Macrochemical Journal*, **2019**, *149*, 103976
- Shetti, N. P.; Malode, S. J.; Nandibewoor, S. T.; *Analytical Methods*, **2015**, *7*, 8673.
- Lee, S.; Lee, Y. J.; Kim, J. H.; Lee, G. J.; *Chemosensors*, **2020**, *8*, 63.
- Jimenez-Perez, R.; Gonzalez-Rodriguez, J.; Gonzalez-Sanchez, M. I.; Gomez-Monedero, B.; Valero E.; *Sens. Actuators B Chem.*, **2019**, *298*, 126878.
- Long, L.; Liu, H.; Liu, X.; Chen, L.; Wang, S.; Liu, C.; Dong, S.; Jia, J.; *Sens. Actuators B Chem.*, **2020**, *318*, 128242.
- Han, L.; Cui, S.; Deng, D.; Li, Y.; Yan, X.; He, H.; Luo, L.; *Current Anal. Chem.*, **2020**, *16*, 485.
- Jia, W.; Guo, M.; Zheng, Z.; Yu, T.; Rodriguez, E. G.; Wang, Y.; Lei, Y.; *Journal of Electroanalytical Chemistry*, **2009**, *625*, 27.
- Fang, K.; Yang, Y.; Fu, L.; Zheng, H.; Yuan, J.; Niu, L.; *Sensors and Actuators B*, **2014**, *191*, 401.
- Ampelli, C.; Leonardi, S. G.; Bonavita, A.; Genovese, C.; Papanikolaou, G.; Perathoner, S.; Centi G.; *Neri Chemical Engineering Transactions*, **2015**, *43*, 733.
- Kitte, S. A.; Assreshegn, B. D.; Soreta, T. R.; *J. Serb. Chem. Soc.* **2013**, *78*, 701.

- Li, Y.; Cheng, Y.; Jin, M.; Iui, Y.; Han, G.; *Journal of Applied Polymer Science*, **2012**, *126*, 1316.
- Scandurra, G.; Arena, A.; Ciofi, C.; Saitta G.; *Sensors*, **2013**, *13*, 3878.
- Teranishi, T.; Miyake, M.; *Chem. Mater.* **1998**, *10*, 594.
- Hanemann, S.; Grunwalat, J.D.; Krumeich, F.; Kappen, P.; Baiker, A.; *Appl. Surf. Sci.*, **2006**, *252*, 7862.
- Borghain, K.; Murase, N.; Mahamuni, S.; *J. Apply. Phy.* **2002**, *92*, 1294.

### Authors biography



**Dr. Nitin Dighore** is Assistance Professor, S. N. Mor College Tumsar, Dist. Bhandara, M.S. He obtained Ph.D. in Chemistry from Dr. Babasaheb Ambedkar Marathwada University, Aurangabad in 2017. He carried out research worked on synthesis of metal/metal oxide nanoparticles as catalytic and biological activity. His work is focused on the synthesis of metal nanoparticles and conducting polymer naocomposites as electrochemical sensors.



**Ms. Priya Dahare** is work as lecturer MPL Nehru Junior College Tumsar Ta. Tumsar Dist. Bhandara. She obtained M.Sc. degree in Chemistry from Dr. Babasaheb Ambedkar Marathwada University, Aurangabad in 2017. Her research interest synthesis metal/metal oxide nanoparticles as electrochemical biosensor



**Prof. Capt. Suresh Gaikwad** is a Professor, Department of Chemistry at the Dr. Babasaheb Ambedkar Marathwada University, Aurangabad, India. He obtained a Ph.D. in Chemistry in 2007 at Dr. Babasaheb Ambedkar Marathwada University, Aurangabad in India. His research interests include synthesis of biologically active meal complexes, metal nanoparticles. He has published number of papers in the area of coordination chemistry, catalysis, material science and antimicrobial activity of metal complexes.



**Prof. Anjali Rajbhoy** is a Professor, Department of Chemistry at the Dr. Babasaheb Ambedkar Marathwada University, Aurangabad, India. She obtained a Ph.D. in Chemistry in 2004 at Dr. Babasaheb Ambedkar Marathwada University, Aurangabad in India. Her research interests include synthesis of metal nanoparticles, conducting polymer naocomposite and metal complexes. She has published number of papers in the area of coordination chemistry, material science, catalysis and antimicrobial activity.

### Supporting information

**Scheme 1.** Structure of poly(3 acetyl pyrrole-co-pyrrole)-WO<sub>3</sub> nanocomposites.

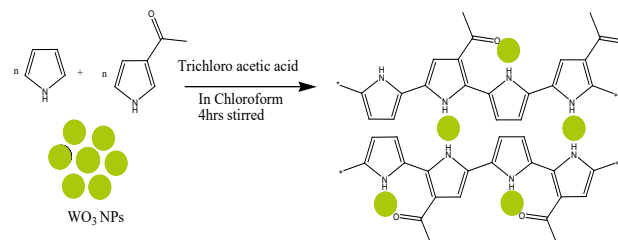


**Table S1.** XRD analysis data of PPAP-WO<sub>3</sub> NCPs.

2θ	d (Å)	Height	Area	FWHM
16.443	5.386	869	63850	0.7138
23.057	3.854	56.7	6792	0.6534
24.217	3.672	287.7	34269	0.6534
26.711	3.334	73	11259	0.5803
27.087	2.289	71.6	8148	0.9259
34.803	2.575	506	48477	0.7344
38.540	2.334	123	15539	0.9393
46.717	1.942	47.2	4131	0.3108
49.577	1.837	315	27046	0.4391
52.653	1.736	212	15394	0.7007
56.874	1.617	155	19355	0.9354